Gould, P.L. and Kratzig, W.B. “Cooling Tower Structures”
Structural Engineering Handbook
Ed. Chen Wai-Fah
Boca Raton: CRC Press LLC, 1999

Cooling Tower Structures

Phillip L. Gould
Department of Civil Engineering,
Washington University,
St. Louis, MO

Wilfried B. Krätzig
Ruhr-University,
Bochum, Germany

14.1 Introduction

Hyperbolic cooling towers are large, thin shell reinforced concrete structures which contribute to environmental protection and to power generation efficiency and reliability. As shown in Figure 14.1, they may dominate the landscape but they possess a certain aesthetic .eloquence due to their doubly curved form. The operation of a cooling tower is illustrated in Figure 14.2. In a thermal power station, heated steam drives the turbogenerator which produces electric energy. To create an efficient heat sink at the end of this process, the steam is condensed and recycled into the boiler. This requires a large amount of cooling water, whose temperature is raised and then recooled in the tower.

In a so-called "wet" natural draft cooling tower, the heated water is distributed evenly through channels and pipes above the fill. As the water flows and drops through the fill sheets, it comes into contact with the rising cooler air. Evaporative cooling occurs and the cooled water is then collected in the water basin to be recycled into the condenser. The difference in density of the warm air inside and the colder air outside creates the natural draft in the interior. This upward flow of warm air, which leads to a continuous stream of fresh air through the air inlets into the tower, is protected against atmospheric turbulence by the reinforced concrete shell. The cooling tower shell is supported by a truss or framework of columns bridging the air inlet to the tower foundation.

There are also "dry" cooling towers that operate simply on the basis of convective cooling. In this case the water distribution, the fill, and the water basin are replaced by a closed piping system around the air inlet, resembling, in fact, a gigantic automobile radiator. While dry cooling towers are doubtless superior from the point of view of environmental protection, their thermal efficiency is only about 30% of comparable wet towers. If the flue gas is cleaned by a washing technology, it is frequently discharged into the atmosphere by the cooling tower upward flow. This saves reheating of the cleaned flue gas and the construction of a smoke stack (see Figure 14.2).

Figure 14.3 summarizes the historical development of natural draft cooling towers. Technical cooling devices first came into use at the end of the 19th century. The well-known hyperbolic shape

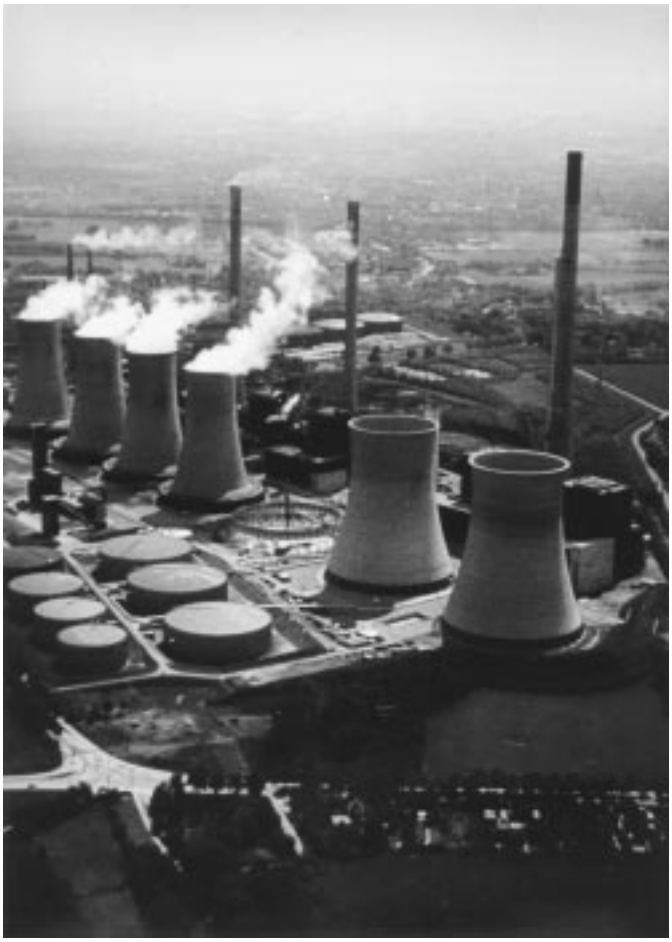

FIGURE 14.1: A group of hyperbolic cooling towers.

of cooling towers was introduced by two Dutch engineers, Van Iterson and Kuyper, who in 1914 constructed the first hyperboloidal towers which were 35 m high. Soon, capacities and heights increased until around 1930, when tower heights of 65 m were achieved. The first such structures to reach higher than 100 m were the towers of the High Marnham Power Station in Britain.

Today's tallest cooling towers, located at several EDF nuclear power plants in France, reach heights of about 170 m. The key dimensions of one of the largest modern towers are shown in Figure 14.4. In relative proportions, the shell is thinner than an egg, and it is predicted that 200 m high towers will be constructed in the early 21st century.

14.2 Components of a Natural Draft Cooling Tower

The most prominent component of a natural draft cooling tower is the huge, towering shell. This shell is supported by diagonal, meridional, or vertical columns bridging the air inlet. The columns, made of high-strength reinforced concrete, are either prefabricated or cast *in situ* into moveable steel forms (Figure 14.5). After the erection of the ring of columns and the lower edge member, the climbing formwork is assembled and the stepwise climbing construction of the cooling tower shell

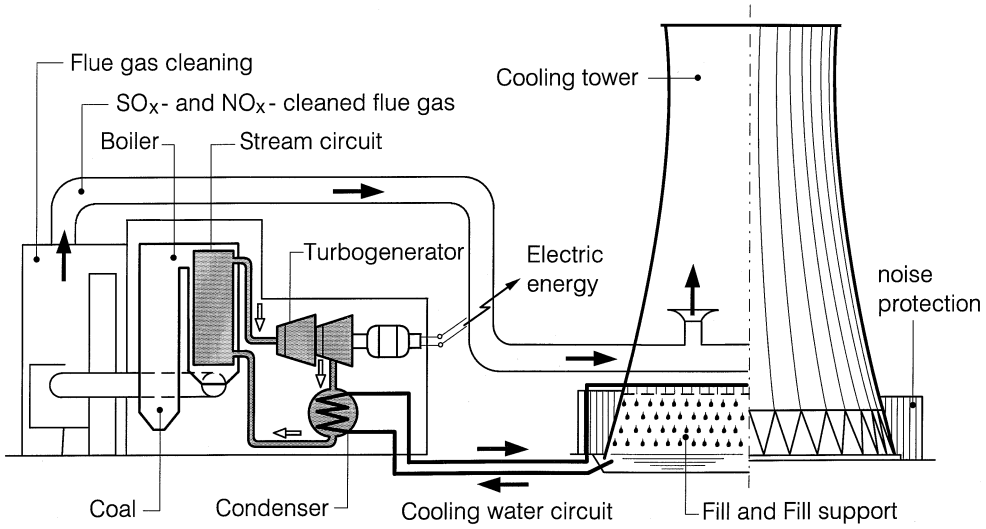

FIGURE 14.2: Thermal power plant with cleaned flue gas injection.

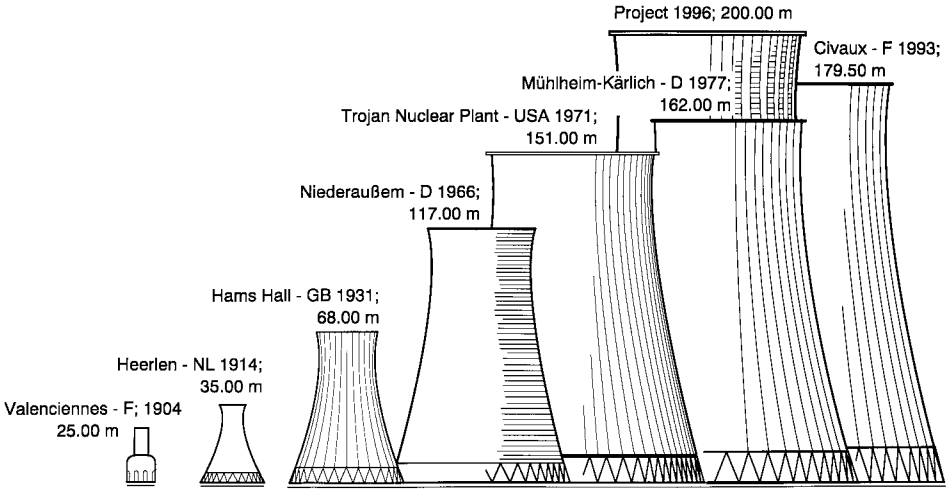

FIGURE 14.3: Historical development of natural draft cooling tower.

begins (Figure 14.6a). Fresh concrete and reinforcement steel are supplied to the working site by a central crane anchored to the completed parts of the shell, and are placed in lifts up to 2 m high (Figure 14.6b). After sufficient strength has been gained, the complete forms are raised for the next lift.

To enhance the durability of the concrete and to provide sufficient cover for the reinforcement, the cooling tower shell thickness should not be less than 16 to 18 cm. The shell itself should be sufficiently stiffened by upper and lower edge members. In order to achieve sufficient resistance against instability, large cooling tower shells may be stiffened by additional internal or external rings. These stiffeners may also serve as a repair or rehabilitation tool.

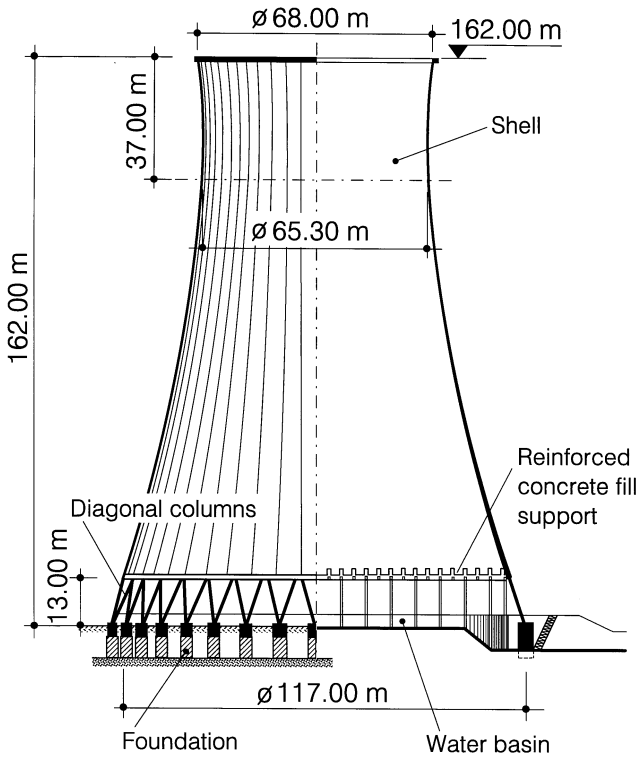

FIGURE 14.4: Cooling tower: Gundremmingen, Germany.

Wet cooling towers have a water basin with a cold water outlet at the base. These are both large engineered structures, able to handle up to 50 m^3/s of water circulation, as indicated in Figure 14.7. The fill construction inside the tower is a conventional frame structure, always prefabricated. It carries the water distribution, a large piping system, the spray nozzles, and the fill-package. Often dripping traps are applied on the upper surfaces of the fill to keep water losses through the uplift stream under 1%. Finally, noise protection elements around the inlet decrease the noise caused by the continuously dripping water, as illustrated in Figure 14.2.

14.3 Damage and Failures

Today's natural draft cooling towers are safe and durable structures if properly designed and constructed. Nevertheless, it should be recognized that this high quality level has been achieved only after the lessons learned from a series of collapsed or heavily damaged towers have been incorporated into the relevant body of engineering knowledge.

While cooling towers have been the largest existing shell structures for many decades, their design and construction were formerly carried out simply by following the existing "recognized rules of craftsmanship", which had never envisaged constructions of this type and scale. This changed radically, however, in the wake of the Ferrybridge failures in 1965 [7]. On November 1st, 1965, three of eight 114 m high cooling towers collapsed during a Beaufort 12 gale in an obviously identical manner (Figure 14.8). Within a few years of this spectacular accident, the response phenomena of cooling towers had been studied in detail, and safety concepts with improved design rules were developed. These international research activities gained further momentum after the occurrence of failures in

FIGURE 14.5: Fabrication of supporting columns.

Ardeer (Britain) in 1973, Bouchain (France) in 1979, and Fiddler's Ferry (Britain) in 1984, the latter case clearly displaying the influence of dynamic and stability effects.

In surveying these failures, one can recognize at least four common circumstances:

1. The maximum design wind speed was often underestimated, so that the safety margin for the wind load was insufficient.
2. Group effects leading to higher wind speeds and increased vortex shedding influence on downstream towers were neglected.
3. Large regions of the shell were reinforced only in one central layer (in two orthogonal directions), or the double layer reinforcement was insufficient.
4. The towers had no upper edge members or the existing members were too weak for stiffening the structure against dynamic wind actions.

Two towers in the U.S., namely at Willow Island, West Virginia, and at Port Gibson, Mississippi, were heavily damaged during their construction stage, the latter by a tornado. The Port Gibson tower was repaired partly by adding intermediate ring stiffeners [5]. Another tower in Poland collapsed without any definitive explanation having been published up to now, but probably because of considerable imperfections.

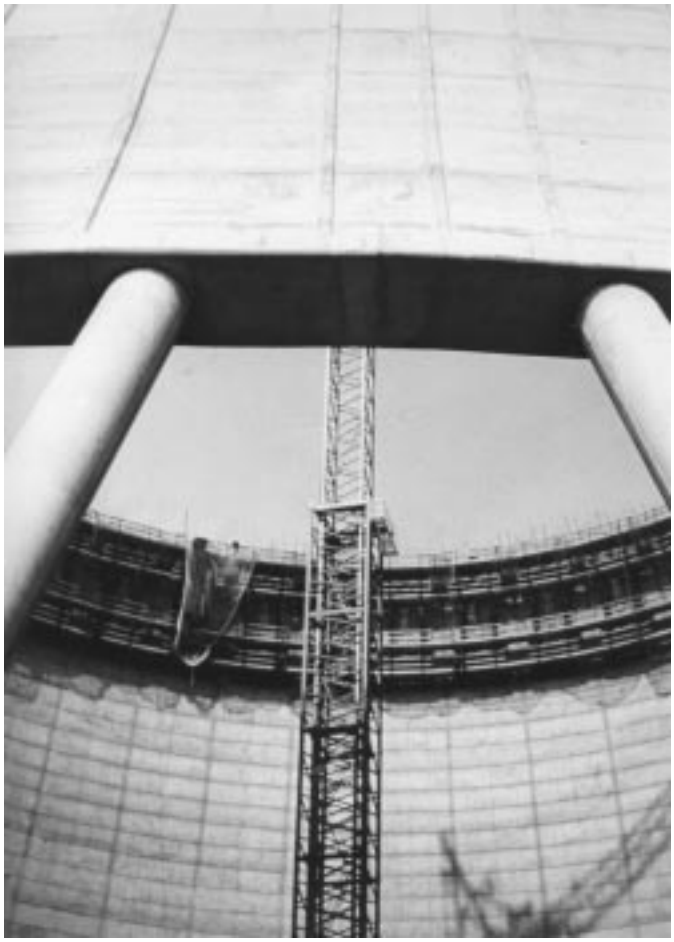

FIGURE 14.6: Climbing construction of the shell.

In addition to these cases, cracking of many cooling towers has been observed, often due to ground motions following underground coal mining, or just because of faulty design and construction. Obviously, any visible crack in a cooling tower shell is an indication of deterioration of its safety and reliability. It is thus imperative to conform to a design concept that guarantees sufficiently safe and reliable structures over a predetermined lifetime.

Although power plant construction over much of the industrialized west has slowed in the last decade, research and development on the structural aspects of hyperbolic cooling towers has continued [4, 9] and a new wave of construction for these impressive structures seems to be approaching. Engineers face this challenge with confidence in their improved analytical tools, in their ability to employ improved materials, and in their valuable experience in construction.

14.4 Geometry

The main elements of a cooling tower shell in the form of a hyperboloid of revolution are shown in Figure 14.9. This form falls into the class of structures known as thin shells. The cross-section as shown depicts the ideal profile of a shell generated by rotating the hyperboloid $R = f(Z)$ about

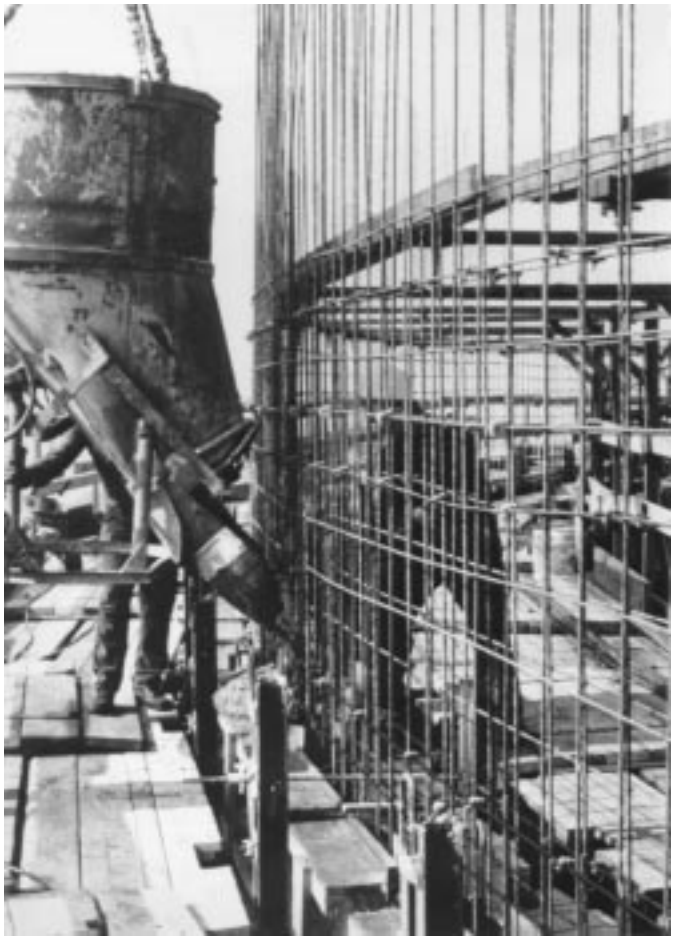

FIGURE 14.6 Steel reinforcement of shell wall.

the vertical (Z) axis. The coordinate Z is measured from the throat while z is measured from the base. All dimensions in the R-Z plane are specified on a reference surface, theoretically the middle surface of the shell but possibly the inner or outer surface. Dimensions through the thickness are then referred to this surface. There are several variations possible on this idealized geometry such as a cone-toroid with an upper and lower cone connected by a toroidal segment, two hyperboloids with different curves meeting at the throat, and an offset of the curve describing the shell wall from the axis of rotation.

Important elements of the shell include the *columns* at the base, which provide the necessary opening for the air; the *lintel*, either a discrete member or more often a thickened portion of the shell, which is designed to distribute the concentrated column reactions into the shell wall; the *shell wall* or *veil*, which may be of varying thickness and provides the enclosure; and the *cornice*, which like the lintel may be discrete or a thickened portion of the wall designed to stiffen the top against ovaling.

Referring to Figure 14.9, the equation of the generating curve is given by

$$4R^2/d_T^2 - Z^2/b^2 = 1 \tag{14.1}$$

FIGURE 14.7: Water basin.

where b is a characteristic dimension of the shell that may be evaluated by

$$b = d_H Z_H / \sqrt{\left(d_H^2 - d_T^2\right)} \tag{14.2}$$

or by

$$b = d_U Z_U / \sqrt{\left(d_U^2 - d_T^2\right)} \tag{14.3}$$

if the upper and lower curves are different. The dimension b is related to the slope of the asymptote of the generating hyperbola (see Figure 14.9) by

$$b = 2cd_T \tag{14.4}$$

14.5 Loading

Hyperbolic cooling towers may be subjected to a variety of loading conditions. Most commonly, these are dead load (D), wind load (W), earthquake load (E), temperature variations (T), construction loads (C), and settlement (S). For the proportioning of the elements of the cooling tower, the effects of the various loading conditions should be factored and combined in accordance with the applicable codes or standards. If no other codes or standards specifically apply, the factors and combinations given in ASCE 7 [11] are appropriate.

Dead load consists of the self-weight of the shell wall and the ribs, and the superimposed load from attachments and equipment.

Wind loading is extremely important in cooling tower design for several reasons. First of all, the amount of reinforcement, beyond a prescribed minimum level, is often controlled by the *net difference* between the *tension* due to wind loading and the dead load *compression*, and is therefore

FIGURE 14.8: Collapse of Ferrybridge Power Station shell.

especially sensitive to variations in the tension. Second, the quasistatic velocity pressure on the shell wall is sensitive to the vertical variation of the wind, as it is for most structures, and also to the circumferential variation of the wind around the tower, which is peculiar to cylindrical bodies. While the vertical variation is largely a function of the regional climatic conditions and the ground surface irregularities, the circumferential variation is strongly dependent on the roughness properties of the shell wall surface. There are also additional wind effects such as internal suction, dynamic amplification, and group configuration.

The external wind pressure acting at any point on the shell surface is computed as [2, 9]

$$q(z,\theta) = q(z)H(\theta)(1+g) \tag{14.5}$$

in which

$q(z)$ = effective velocity pressure at a height z above the ground level (Figure 14.9)
$H(\theta)$ = coefficient for circumferential distribution of external wind pressure
$1+g$ = gust response factor
g = peak factor

As mentioned above, $q(z)$ should be obtained from applicable codes or standards such as Reference [11].

The circumferential distribution of the wind pressure is denoted by $H(\theta)$ and is shown in Figure 14.10. The key regions are the windward meridian, $\theta = 0°$, the maximum side suction, $\theta \simeq 70°$, and the back suction, $\theta \geq 90°$. These curves were determined by laboratory and field measurements as a function of the roughness parameter k/a as shown in Figure 14.11, in which k is the height of

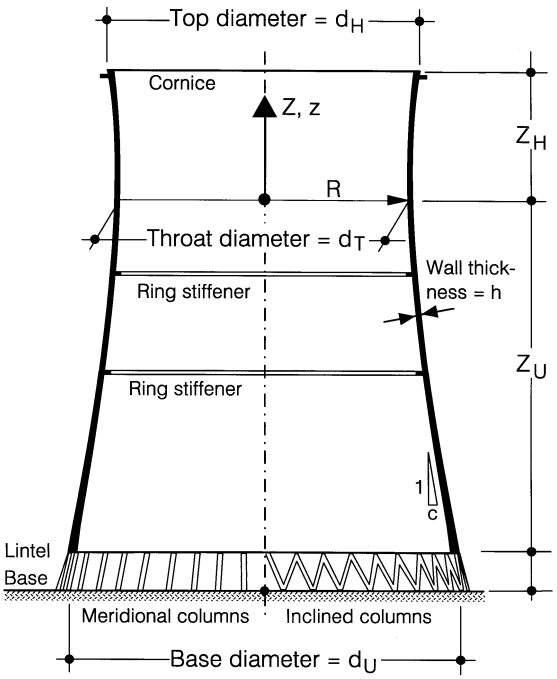

FIGURE 14.9: Hyperbolic cooling tower.

the rib and a is the mean distance between the ribs measured at about 1/3 of the height of the tower. Note that the coefficient along the windward meridian $H(0)$ reflects the so-called *stagnation pressure* while the side-suction is, remarkably, significantly affected by the surface roughness k/a. As will be discussed in a later section, the meridional forces in the shell wall and hence the required reinforcing steel are very sensitive to $H(\theta)$. In turn, the costs of construction are affected. Thus, the design of the ribs, or of alternative roughness elements, are an important consideration. For quantitative purposes, the equations of the various curves are given in Table 14.1 and tabulated values at 5° intervals are available [13].

TABLE 14.1 Functions of Pressure Curves $H(\Theta)$ and Corresponding Drag Coefficients c_W

Curve	Minimum pressure	Area I	Area II	Area III	c_W
K1.0	−1.0	$1-2.0\left(\sin\frac{90}{70}\Theta\right)^{2.267}$	$-1.0+0.5\left[\sin\left[\frac{90}{21}(\Theta-70)\right]\right]^{2.395}$	−0.5	0.66
K1.1	−1.1	$1-2.1\left(\sin\frac{90}{71}\Theta\right)^{2.239}$	$-1.1+0.6\left[\sin\left[\frac{90}{22}(\Theta-71)\right]\right]^{2.395}$	−0.5	0.64
K1.2	−1.2	$1-2.2\left(\sin\frac{90}{72}\Theta\right)^{2.205}$	$-1.2+0.7\left[\sin\left[\frac{90}{23}(\Theta-72)\right]\right]^{2.395}$	−0.5	0.60
K1.3	−1.3	$1-2.3\left(\sin\frac{90}{73}\Theta\right)^{2.166}$	$-1.3+0.8\left[\sin\left[\frac{90}{24}(\Theta-73)\right]\right]^{2.395}$	−0.5	0.56

The circumferential distribution of the external wind pressure may be presented in another manner which accents the importance of the asymmetry. If the distribution $H(\theta)$ is represented in a Fourier cosine series of the form

$$H(\theta) = \sum_{n=0}^{n=\infty} A_n \cos n\theta \tag{14.6}$$

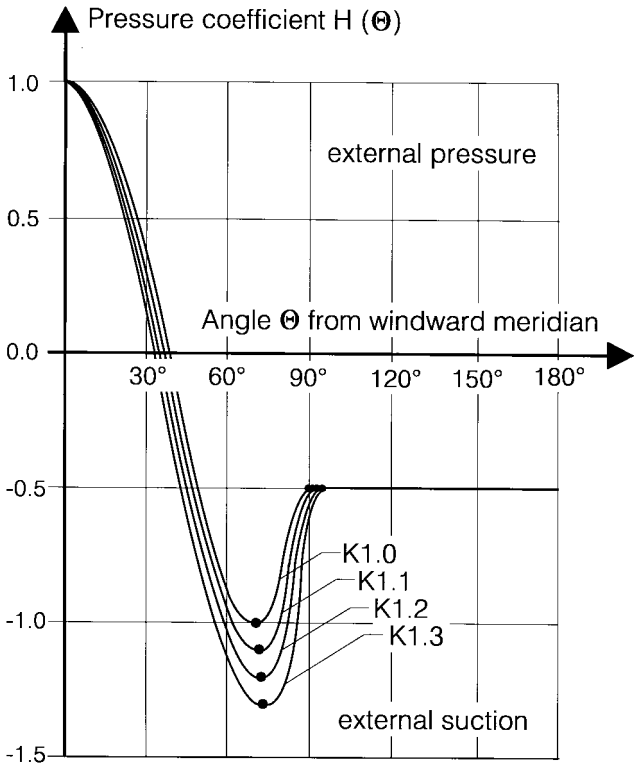

FIGURE 14.10: Types of circumferential pressure distribution.

the Fourier coefficients A_n for a distribution most similar to the curve for K1.3 are as follows [13]:

n	A_n
0	−0.3922
1	0.2602
2	0.6024
3	0.5046
4	0.1064
5	−0.0948
6	−0.0186
7	0.0468

Representative modes are shown in Figure 14.12. The $n = 0$ mode represents uniform expansion and contraction of the circumference, while n =1 corresponds to beam-like bending about a diametrical axis resulting in translation of the cross-section. The higher modes $n > 1$ are peculiar to shells in that they produce undulating deformations around the cross-section with no net translation. The relatively large Fourier coefficients associated with n = 2,3,4,5 indicate that a significant portion of the loading will cause shell deformations in these modes. In turn, the corresponding local forces are significantly higher than a beam-like response would produce.

To account for the internal conditions in the tower during operation, it is common practice to add an axisymmetric internal suction coefficient $H = 0.5$ to the external pressure coefficients $H(\theta)$. In terms of the Fourier series representation, this would increase A_0 to -0.8922.

The dynamic amplification of the effective velocity pressure is represented by the parameter g in Equation 14.5. This parameter reflects the resonant part of the response of the structure and may be as much as 0.2 depending on the dynamic characteristics of the structure. However, when the basis

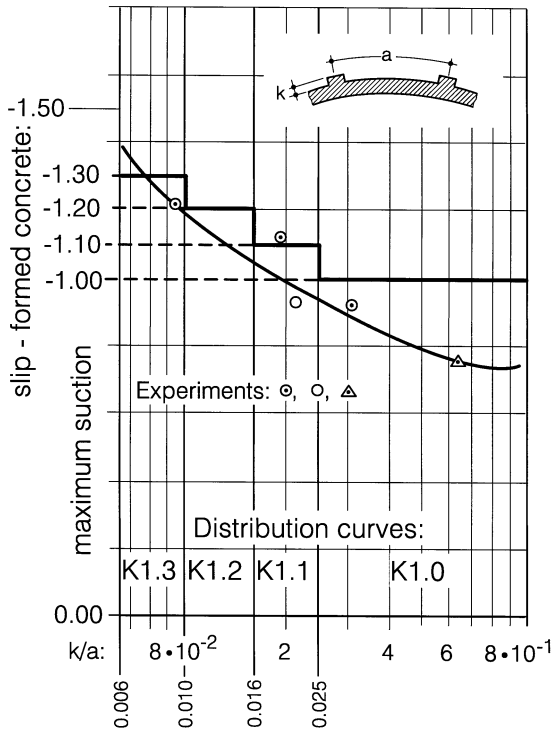

FIGURE 14.11: Surface roughness k/a and maximum side-suction.

of $q(z)$ includes some dynamic portion, such as the fastest-mile-of-wind, $(1+g)$ is commonly taken as 1.0.

Cooling towers are often constructed in groups and close to other structures, such as chimneys or boiler houses, which may be higher than the tower itself. When the spacing of towers is closer than 1.5 times the base diameter or 2 times the throat diameter, or when other tall structures are nearby, the wind pressure on any single tower may be altered in shape and intensity. Such effects should be studied carefully in boundary-layer wind tunnels in order not to overlook dramatic increases in the wind loading.

Earthquake loading on hyperbolic cooling towers is produced by ground motions transmitted from the foundation through the supporting columns and the lintel into the shell. If the base motion is assumed to be uniform vertically and horizontally, the circumferential effects are axisymmetrical ($n = 0$) and antisymmetrical ($n = 1$), respectively (see Figure 14.12). In the meridional direction, the magnitude and distribution of the earthquake-induced forces is a function of the mass of the tower and the dynamic properties of the structure (natural frequencies and damping) as well as the acceleration produced by the earthquake at the base of the structure. The most appropriate technique for determining the loads applied by a design earthquake to the shell and components is the response spectrum method which, in turn, requires a free vibration analysis to evaluate the natural frequencies [2, 3, 4]. It is common to use elastic spectra with 5% of critical damping. The supporting columns and foundation are critical for this loading condition and should be modeled in appropriate detail [3, 4].

Temperature variations on cooling towers arise from two sources: operating conditions and sunshine on one side. Typical operating conditions are an external temperature of $-15°$C and internal temperature of $+30°$C. This is an axisymmetrical effect, $n = 0$ on Figure 14.12. For sunshine, a

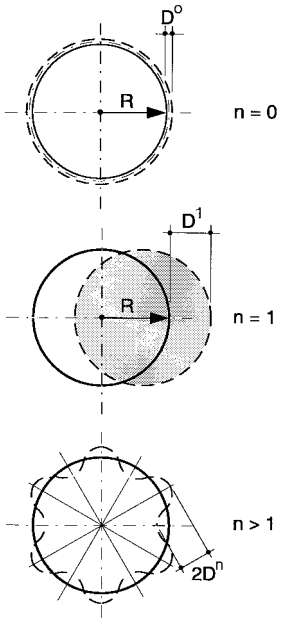

FIGURE 14.12: Harmonic components of the radial displacement.

temperature gradient of 25°C constant over the height and distributed as a half-wave around one half of the circumference is appropriate. This loading would require a Fourier expansion in the form of Equation 14.6 and higher harmonic components, $n > 1$, to be considered.

Construction loads are generally caused by the fixing devices of climbing formwork, by tower crane anchors, and by attachments for material transport equipment as shown in Figure 14.13. These loads must be considered on the portion of the shell extant at the phase of construction.

Non-uniform settlement due to varying subsoil stiffness may be a consideration. Such effects should be modeled considering the interaction of the foundation and the soil.

14.6 Methods of Analysis

Thin shells may resist external loading through forces acting parallel to the shell surface, forces acting perpendicular to the shell surface, and moments. While the analysis of such shells may be formulated within the three-dimensional theory of elasticity, there are reduced theories which are two-dimensional and are expressed in terms of force and moment *intensities*. These intensities are traditionally based on a reference surface, generally the middle surface, and are forces and moments per unit length of the middle surface element upon which they act. They are called *stress resultants* and *stress couples*, respectively, and are associated with the three directions: circumferential, θ^1; meridional, θ^2; and normal, θ^3. In Figure 14.14, the extensional stress resultants, n_{11} and n_{22}, the in-plane shearing stress resultants, $n_{12} = n_{21}$, and the transverse shear stress resultants, $q_{12} = q_{21}$, are shown in the left diagram along with the components of the applied loading in the circumferential, meridional, and normal directions, p_1, p_2, and p_3, respectively. The bending stress couples, m_{11} and m_{22}, and the twisting stress couples, $m_{12} = m_{21}$, are shown in the right diagram along with the displacements v_1, v_2, and v_3 in the respective directions.

Historically, doubly curved thin shells have been designed to resist applied loading primarily through the extensional and shearing forces in the "plane" of the shell surface, as opposed to the

FIGURE 14.13: Attachments on shell wall.

transverse shears and bending and twisting moments which predominate in flat plates loaded normally to their surface. This is known as *membrane* action, as opposed to *bending* action, and is consistent with an accompanying theory and calculation methodology which has the advantage of being statically determinate. This methodology was well-suited for the pre-computer age and enabled many large thin shells, including cooling towers, to be rationally designed and economically constructed [9]. Because the conditions that must be provided at the shell boundaries in order to insure membrane action are not always achievable, shell bending should be taken into account even for shells designed by membrane theory. Remarkably, the accompanying bending often is confined to narrow regions in the vicinity of the boundaries and other discontinuities and may have only a minor effect on the shell design, such as local thickening and/or additional reinforcement. Many clever and insightful techniques have been developed over the years to approximate the effects of local bending in shells designed by the membrane theory.

As we have passed into and advanced in the computer age, it is no longer appropriate to use the membrane theory to analyze such extraordinary thin shells, except perhaps for preliminary design purposes. The finite element method is widely accepted as the standard contemporary technique and the attention shifts to the level of sophistication to be used in the finite element model. As is often the case, the greater the level of sophistication specified, the more data required. Consequently,

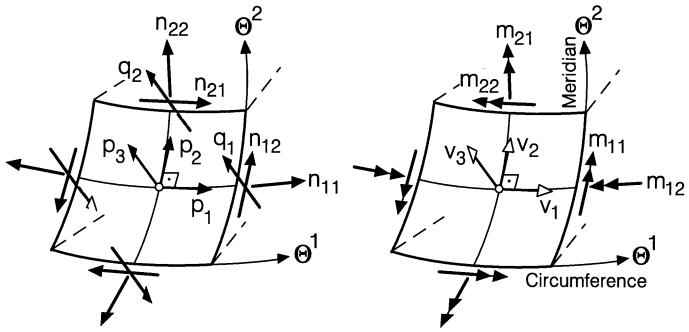

FIGURE 14.14: Surface loads, stress resultants, stress couples, and displacements.

a model may evolve through several stages, starting with a relatively simple version that enables the structure to be sized, to the most sophisticated version that may depict such phenomena as the sequence of progressive collapse of the as-built shell under various static and dynamic loading scenarios, the incremental effects of the progressive stages of construction, the influence of the operating environment, aging and deterioration on the structure, etc. The techniques described in the following paragraphs form a hierarchical progression from the relatively simple to the very complex, depending on the objective of the analysis.

In modeling cooling tower shells using the finite element method, there are a number of options. For the shell wall, ring elements, triangular elements, or quadrilateral elements have been used. Earlier, flat elements adapted from the two-dimensional elasticity and plate formulations were used to approximate the doubly curved surface. Such elements present a number of theoretical and computational problems and are *not* recommended for the analysis of shells. Currently, shell elements degenerated from three-dimensional solid elements are very popular. These elements have been utilized in both the ring and quadrilateral form.

The column region at the base of the shell presents a special modeling challenge. For static analysis, the lower boundary is often idealized as a uniform support at the lintel level. Then, a portion of the lower shell and the columns is considered in a subsequent analysis to account for the concentrated actions of the columns, which may penetrate only a relatively short distance into the shell wall. For dynamic analysis, it is important to include the column region along with the veil in the model. An equivalent shell element has proved useful in this regard if ring elements are used to model the shell [3, 4]. It may also be desirable to include some of the foundation elements, such as a ring beam at the base and even the supporting piles in a dynamic or settlement model.

The linear static analysis method is based on the classical bending theory of thin shells. While this theory has been formulated for many years, solutions for doubly curved shells have not been readily achievable until the development of computer-based numerical methods, most notably the finite element method. The outputs of such an analysis are the stress resultants and couples, defined on Figure 14.14, over the entire shell surface and the accompanying displacements. The analysis is based on the initial geometry, linear elastic material behavior, and a linear kinematic law. Some representative results of such analyses for a large cooling tower (Figure 14.15) are shown in Figures 14.16 through 14.24 for some of the important loading conditions discussed in the preceding section. The finite element model used considers the shell to be fixed at the top of the columns and, thus, does not account for the effect of the concentrated column reactions. Also, in considering the analyses under the individual loading conditions, it should be remembered that the effects are to be factored and combined to produce design values.

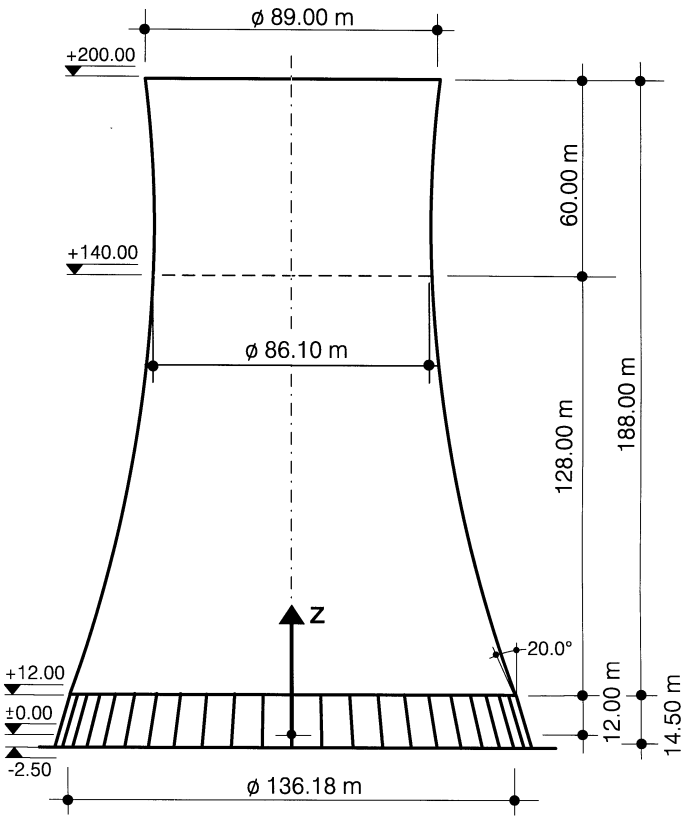

FIGURE 14.15: Design project for a 200-m high cooling tower: geometry.

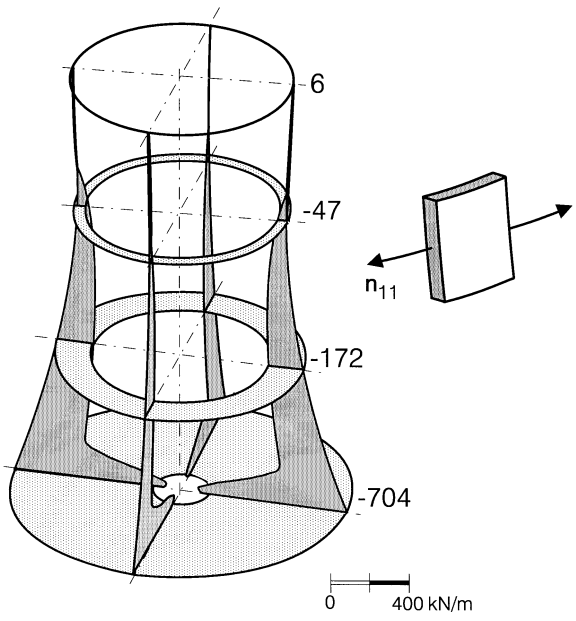

FIGURE 14.16: Circumferential forces n_{11G} under deadweight.

The dead load analysis results in Figures 14.16 and 14.17 indicate that the shell is always under compression in both directions, except for a small circumferential tension near the top. This is a very desirable feature of this geometrical form.

In Figures 14.18 through 14.20, the results of an analysis for a quasistatic wind load using the K1.0 distribution from Figure 14.10 are shown. Large tensions in both the meridional and circumferential directions are present. The regions of tension may extend a considerable distance along the circumference from the windward meridian, and the magnitude of the forces is strongly dependent on the distribution selected. In contrast to bluff bodies, where the magnitude of the extensional force along the meridian would be essentially a function of the overturning moment, the cylindrical-type body is also strongly influenced by the circumferential distribution of the applied pressure, a function of the surface roughness. The major effect of the shearing forces is at the level of the lintel where they are transferred into the columns. The internal suction effects (Figures 14.21 and 14.22) are significant only in the circumferential direction.

For the service temperature case shown in Figures 14.23 and 14.24, the main effects are bending in the lower region of the shell wall.

The analysis of hyperbolic cooling towers for instability or buckling is a subject that has been investigated for several decades [1]. Shell buckling is a complex topic to treat analytically in any case due to the influence of imperfections; for reinforced concrete, it is even more difficult. While the governing equations may be generalized to treat instability by using nonlinear strain-displacement relations and thereby introducing the geometric stiffness matrix, the correlation between the resulting analytical solutions and the possible failure of a reinforced concrete cooling tower is questionable. Nevertheless, it has been common to analyze cooling tower shells under an unfactored combination of dead load plus wind load plus internal suction. The corresponding buckling pattern is shown in Figure 14.25.

Interaction diagrams calibrated from experimental studies based on bifurcation buckling are also available [9, 12, 13]. Additionally, there are empirical methods based on wind tunnel tests that consider a snap-through buckle at the upper edge at each stage of construction [13]. These formulas are proportional to h/R and are convenient for establishing an appropriate shell thickness. If buckling safety is evaluated based on such a linear buckling analysis or an experimental investigation, the buckling safety factor for realistic material parameters should exceed 5.0. Presently, however, the use of bifurcation buckling analyses should be confined to preliminary proportioning since more rational procedures based on nonlinear analysis have been developed to predict the collapse of reinforced concrete shells, as discussed in the following paragraphs.

Advances in the analyses of reinforced concrete have produced the capability to analyze shells taking into account the layered composition of the cross-section as shown in Figure 14.26. Using realistic material properties for steel and for concrete, including tension stiffening in the form shown in Figures 14.27 through 14.29, load-deflection relationships may be constructed for appropriate load combinations. These relationships progress from the linear elastic phase to initial cracking of the concrete through spreading of the cracks until collapse.

Results from a nonlinear study are presented in Figures 14.30 through 14.33. The geometry of the shell is given in Figure 14.30, the wind load factor λ is plotted against the maximum lateral displacement at the top of the shell in Figure 14.31, and the deformed shape for the collapse load is shown in Figure 14.32. Also, the pattern of cracking corresponding to the initial yielding of the reinforcement is indicated in Figure 14.33. For reinforced concrete shells, this type of analysis represents the state-of-the-art and provides a realistic evaluation of the capacity of such shells against extreme loading [8]. Also durability assessments can be performed by this concept, from which particularly weak and crack-endangered regions of the shell can be identified and further reinforced [10].

It is possible to obtain an estimate of the wind load factor, λ, from the results of a linear elastic analysis, even from a calculation based on membrane theory. This estimate is computed as the cracking load for the shell under a combination of $D + \lambda W$ and is predicated on the notion that the

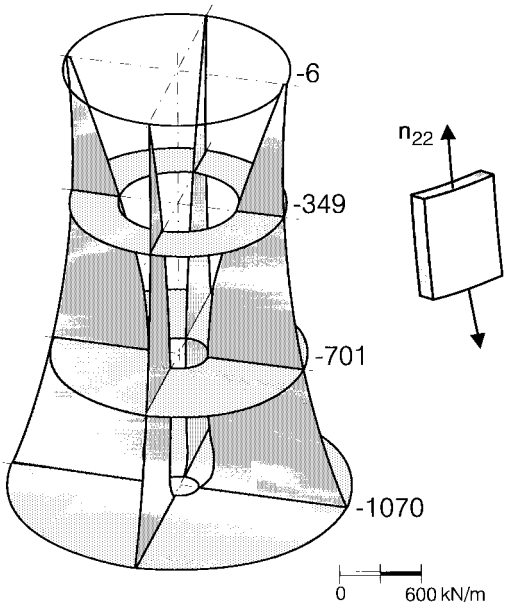

FIGURE 14.17: Meridional forces n_{22G} under deadweight.

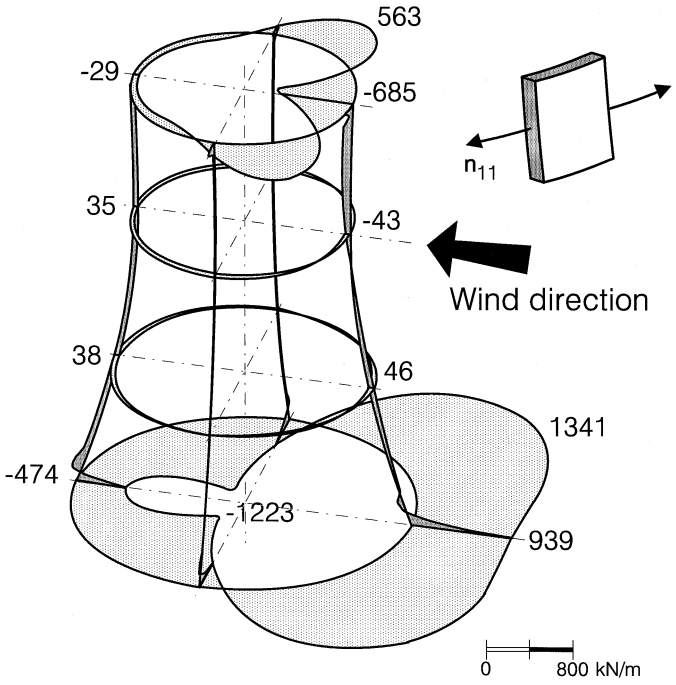

FIGURE 14.18: Circumferential forces n_{11W} under wind load.

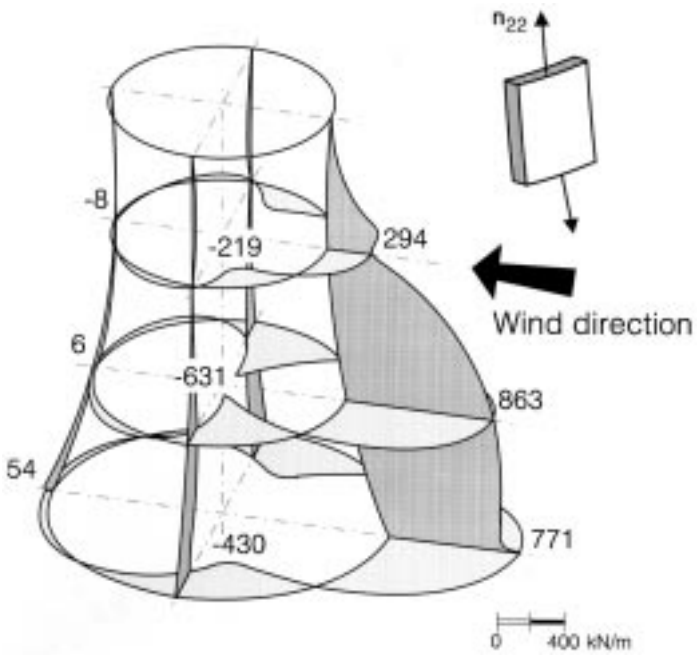

FIGURE 14.19: Meridional forces n_{22W} under wind load.

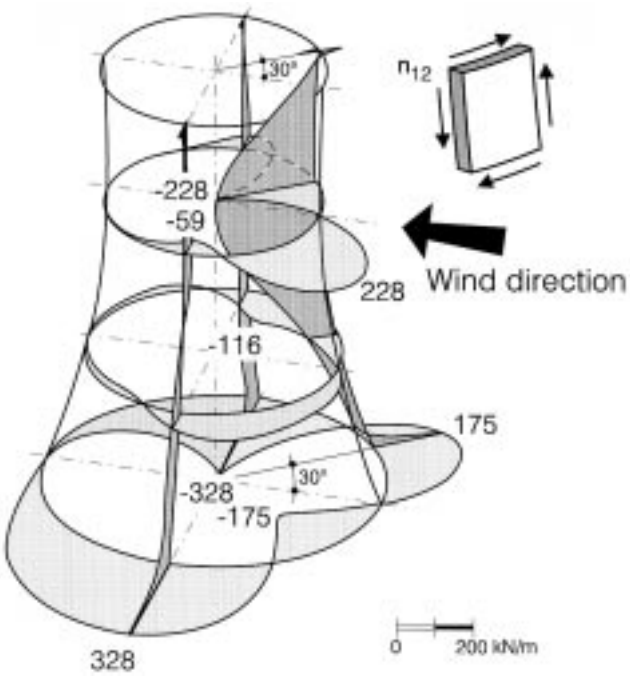

FIGURE 14.20: Shear forces n_{12W} under wind load.

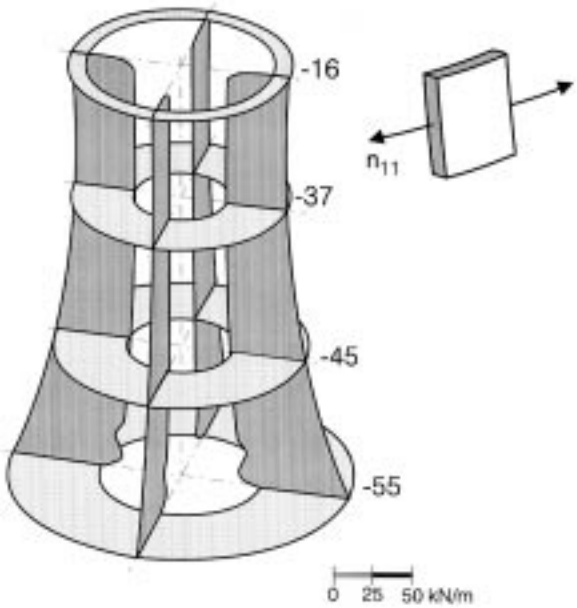

FIGURE 14.21: Circumferential forces n_{11S} under internal suction.

reinforcement may add only a modest amount of capacity to the tower beyond the cracking load [6]. The amount of reinforcement in the wall is often controlled by a specified minimum percentage augmented by that required to resist the net tension due to the factored load combinations. The steel provided is often less than the capacity of the concrete in tension, which is presumed to be lost when the concrete cracks. Therefore, the cracking load represents most of the ultimate capacity of the tower.

The maximum meridional tension location under the wind loading is identified, for example, as the value of $n_{22} = 863$ kN/m in Figure 14.19. The dead load at this location is obtained from Figure 14.17 as -701 kN/m. Taking the concrete tensile capacity as 2,400 kN/m^2 and the wall thickness as 16 cm, the tensile strength is 384 kN/m. Therefore, we have

$$-701 + \lambda 863 = 384 \tag{14.7}$$

giving $\lambda = 1.26$ as the lower bound on the ultimate strength of the tower. Note that the tower used for the linear elastic analysis is much taller than the one shown in Figure 14.30.

The dynamic analysis of cooling towers is usually associated with design for earthquake-induced forces. The most efficient approach is the response spectrum method, but a time history analysis may be appropriate if nonlinearities are to be included [2, 7]. For large shells the dynamic response due to wind is often investigated, at least to determine the positions of the nodal lines and areas of particularly intensive vibrations. In any case the first step is to carry out a free vibration analysis. This analysis represents the modes of free vibration associated with each natural frequency, f, or its inverse the natural period T, as the product of a circumferential mode proportional to $\sin n\theta$ or $\cos n\theta$ and a longitudinal mode along the z axis [3, 4]. Some representative results are shown on Figures 14.34 and 14.35, as discussed below.

As an illustration, the cooling tower from Figure 14.4 is again considered. Some key circumferential and longitudinal modes for a fixed-base boundary condition are shown in Figure 14.35. Also, the effects of different cornice stiffnesses are demonstrated. This model may be regarded as preliminary

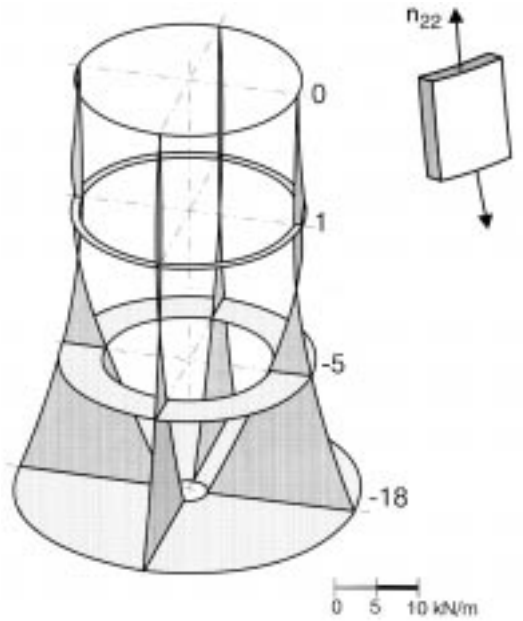

FIGURE 14.22: Meridional forces n_{22S} under internal suction.

in that the relatively soft column supports are not properly represented, but it illustrates the salient characteristics of the modes of vibration. Most interesting are the frequency curves on Figure 14.34 for the first 10 harmonics, also demonstrating the influence of different cornice stiffnesses. Note that the natural frequencies *decrease* with increasing n until a minimum is reached whereupon they increase, a very typical behavior for cylindrical-type shells. Also, the stiffening of the cornice tends to raise the minimum frequency, which is desirable for resistance to dynamic wind. Longitudinally, the cornice stiffness effect is significant for odd modes only.

Specifically for earthquake effects, only the first mode participates in a linear analysis for uniform horizontal base motion and the respective values for $n = 1$ should be entered into the design response spectrum.

Results from a seismic analysis of a cooling tower are presented in Figures 14.36 to 14.39. The cooling tower of Figure 14.4 is subjected to a horizontal base excitation based on Figure 14.36, leading to a first circumferential mode ($n = 1$) participation. A response spectrum analysis provides the lateral displacements w of the tower axis, the meridional forces n_{22}, and the shear forces n_{12} as shown on the indicated figures. In general, cooling tower shells have proven to be reasonably resistant against seismic excitations, but obviously the most critical region is the connection between the columns and the lintel as portrayed in Figure 14.40.

14.7 Design and Detailing of Components

The structural elements of the tower should be constructed with a suitable grade of concrete following the provisions of applicable codes and standards. The design of the mixture should reflect the conditions for placement of the concrete and the external and internal environment of the tower.

The shell wall should be of a thickness which will permit two layers of reinforcement in two perpendicular directions to be covered by a minimum of 3 cm of concrete, and should be no less than 16 cm thick [7, 13]. The buckling considerations mentioned in the previous section have proven to

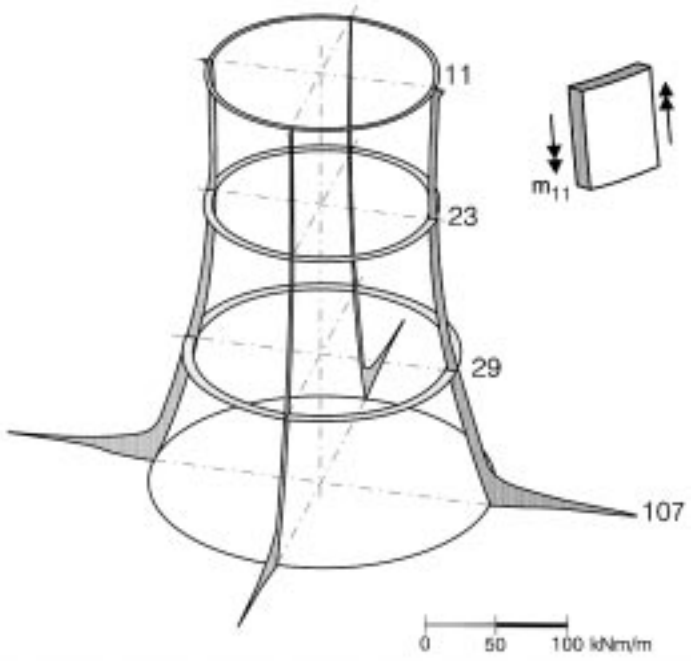

FIGURE 14.23: Circumferential bending moments m_{11T} under service temperature.

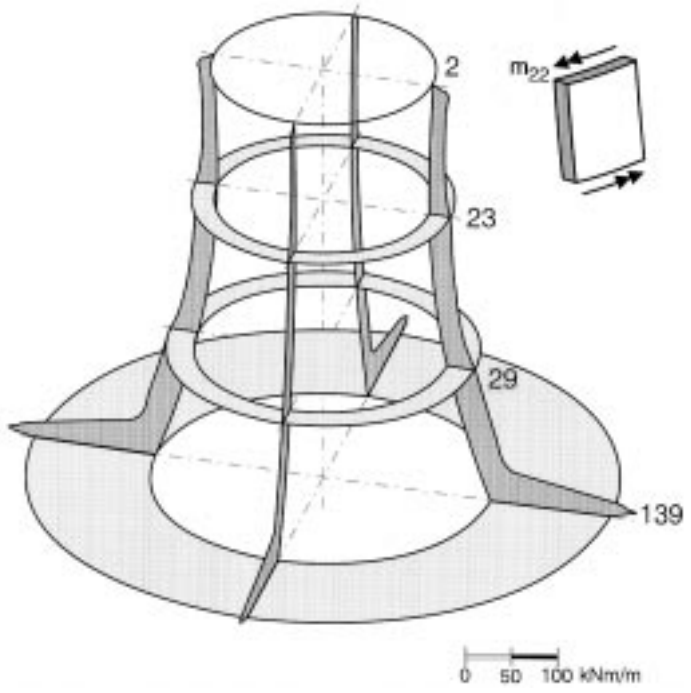

FIGURE 14.24: Meridional bending moments m_{22T} under service temperature.

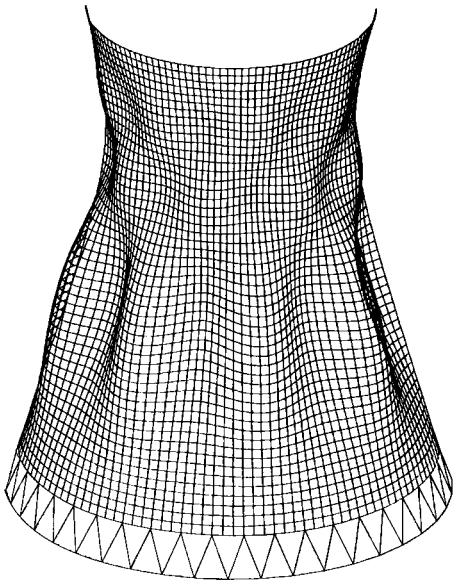

FIGURE 14.25: Buckling pattern of tower shell with upper ring beam: $D + W + S$.

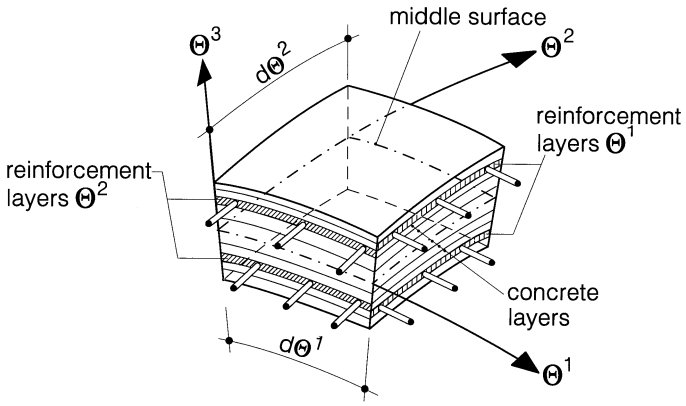

FIGURE 14.26: Layered model for reinforced concrete shell.

be a convenient and evidently acceptable criteria for setting the minimum wall thickness, subject to a nonlinear analysis. The formula

$$q_c = 0.052E(h/R)^{2.3} \tag{14.8}$$

where E = modulus of elasticity, has been used to estimate the critical shell buckling pressure q_c [1, 13]. Then, $h(z)$ is selected to provide a factor of safety of at least 5.0 with respect to the maximum velocity pressure along the windward meridian, $q(z)(1 + g)$. Also, the cornice should have a minimum stiffness of

$$I_x/d_H = 0.0015m^3 \tag{14.9}$$

where I_x is the moment of inertia of the uncracked cross-section about the vertical axis [13]. Some typical forms of the cornice cross-section are shown in Figure 14.41.

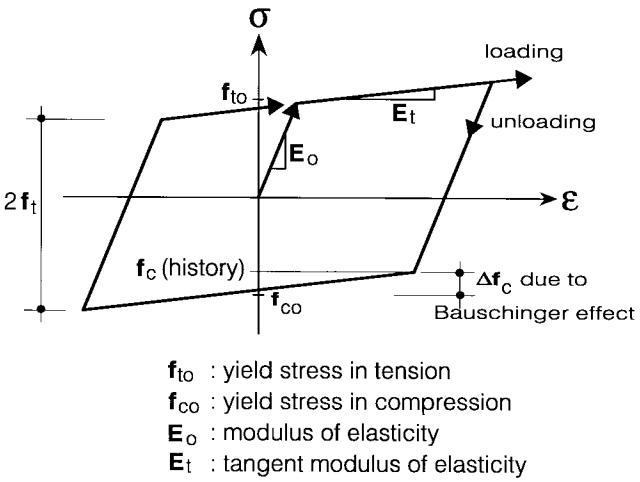

FIGURE 14.27: Elasto-plastic material law for steel.

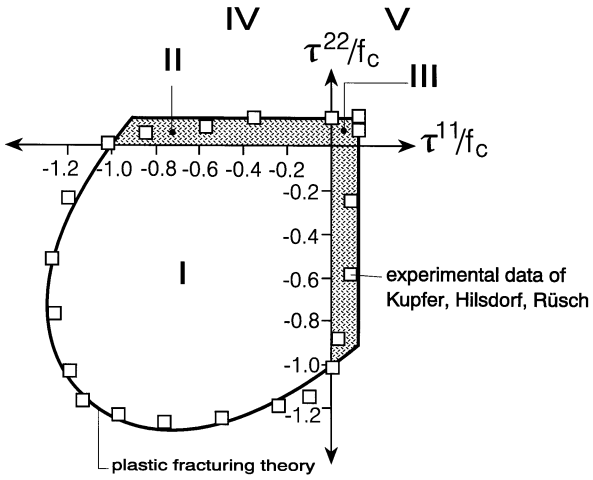

FIGURE 14.28: Biaxial failure envelope of Kupfter/Hilsdorf/Rüsch.

The elements of the cooling tower should be reinforced with deformed steel bars so as to provide for the tensile forces and moments arising from the controlling combination of factored loading cases. The shell walls may be proportioned as rectangular cross-sections subjected to axial forces and bending. As mentioned above, a mesh of two orthogonal layers of reinforcement should be provided in the shell walls, generally in the meridional and circumferential directions [2]. In each direction, the inner and outer layers should generally be the same, except near the edges where the bending may require an unsymmetrical mesh. It is preferable to locate the circumferential reinforcement outside of the meridional reinforcement except near the lintel, where the meridional reinforcement should be on the outside to stabilize the circumferential bars [13]. A typical heavily reinforced segment of the lintel, also showing the anchorage of the column reinforcement into the shell, is depicted in Figure 14.42.

A summary of the most important minimum construction values for the shell wall is given in Figure 14.43 [13]. The bars should not be smaller than 8 mm diameter and, for meridional bars, not

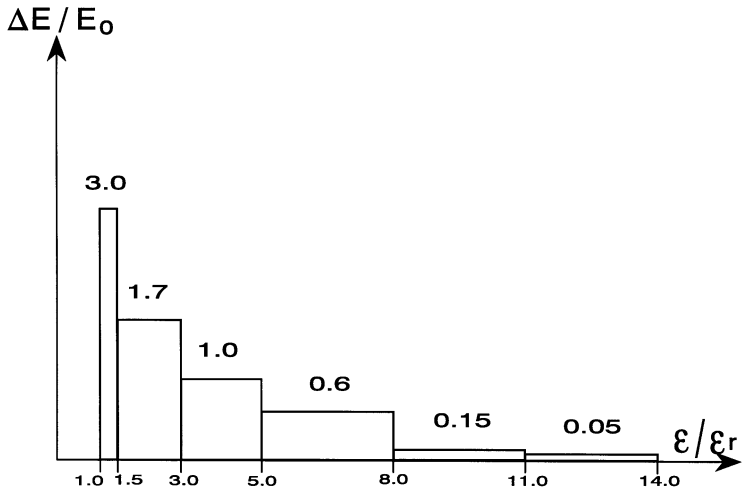

FIGURE 14.29: Additional modulus of elasticity due to tension stiffening.

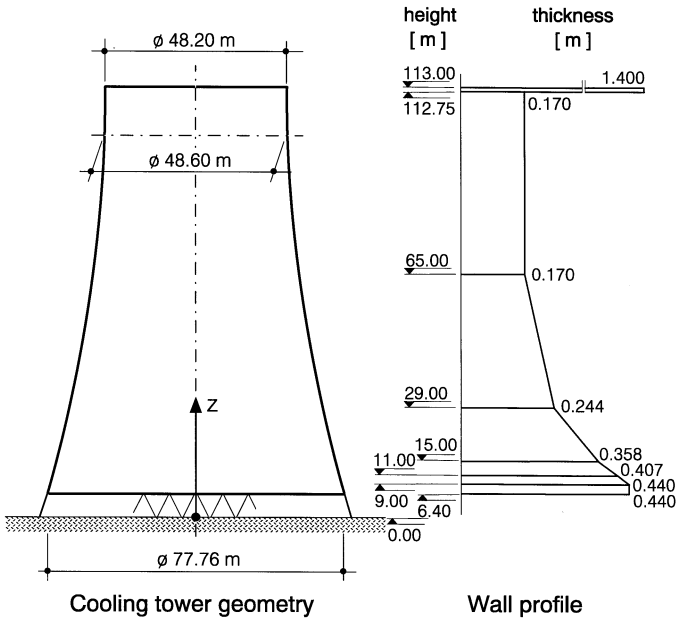

FIGURE 14.30: Shell geometry and wall thickness.

smaller than 10 mm. Further, a minimum of 0.35 to 0.45%, depending on the admissible cracking, should be used in each direction. The minimum cover, as mentioned above, should be 3 cm, the maximum spacing of the bars should be 20 cm, and the splices should be staggered as specified for the construction of walls in the applicable codes or standards. Particular attention should be given to splices in tensile zones.

The supporting columns should ideally be proportioned for the forces and moments computed from an analysis in which they are represented as discrete members, using the appropriate factored loading combinations [3]. If the column region has not been modeled discretely, but rather by a

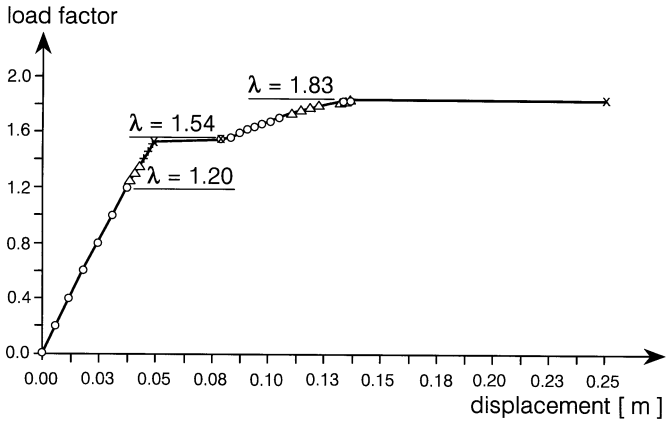

FIGURE 14.31: Load-displacement diagram for load combination $D + \lambda \bullet W$.

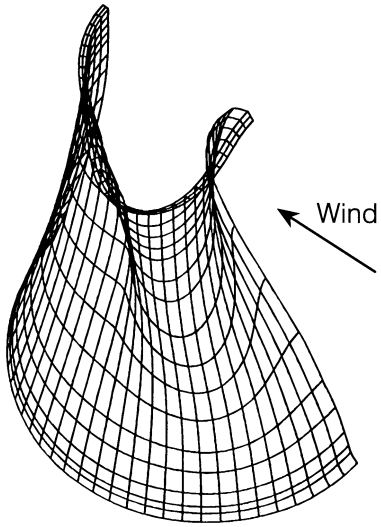

FIGURE 14.32: Displacement plot of the shell for load combination $D + \lambda \bullet W$: load factor $= 1.83$.

continuum approximation, the columns may be proportioned to resist the tributary factored forces and moments at the interface with the lintel, as computed from the shell analysis. The effective length may be taken as unity. Particular attention should be directed toward splices of the column bars when net tension is present. Since large bars will be involved, welded splices are recommended in such regions.

It is possible to add discrete circumferential stiffeners to the shell to increase the stability or to restore capacity that may have been lost due to cracking or other deterioration [5] (see Figure 14.9). Such stiffeners can generally be included in a finite element model of the shell wall and should be proportioned for the forces computed from such an analysis. The eccentricity of the stiffeners with respect to the circumferential axis should be considered when the stiffeners are only on one side of the shell.

The foundations should be proportioned for the factored forces induced by the column reactions, or from the computed forces if the foundation is included in the model with the shell and columns.

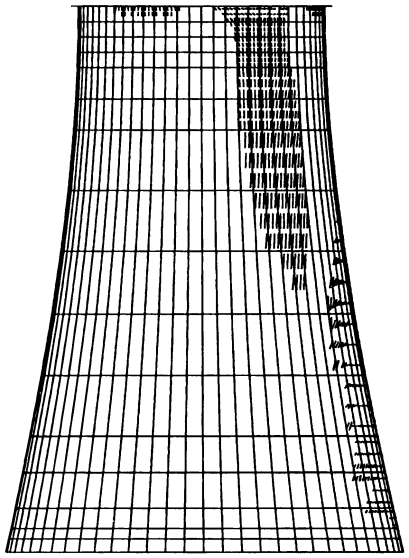

FIGURE 14.33: Crack pattern of the outer face of the shell for load combination $D + \lambda \bullet W$: load factor $= 1.54$.

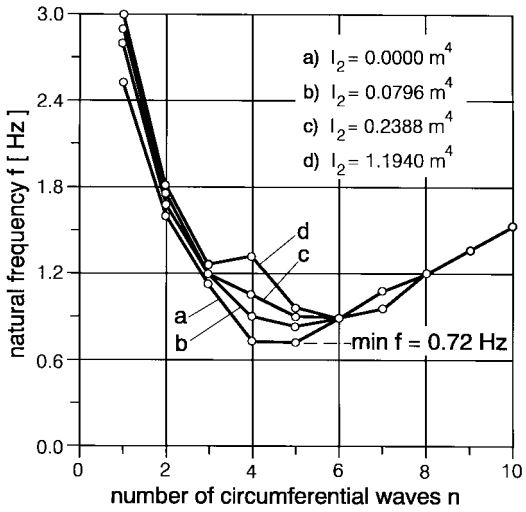

FIGURE 14.34: Natural frequencies for different cornice stiffnesses for the cooling tower on Figure 14.4.

Reinforcement detailing and cover should be in accordance with the applicable codes or standards. Several improved forms for cooling tower foundations have been suggested. Figure 14.44 shows a flat ring footing suitable for uniform soil conditions, while Figure 14.45 portrays a stiff ring beam foundation appropriate for soil conditions that are non-uniform around the circumference. An example of an individual pier on bedrock is given in Figure 14.46.

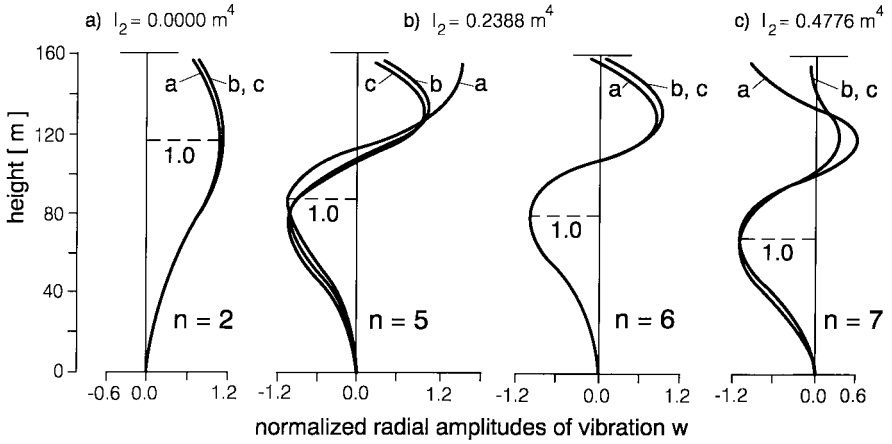

FIGURE 14.35: Normalized natural vibration modes for the cooling tower on Figure 14.4.

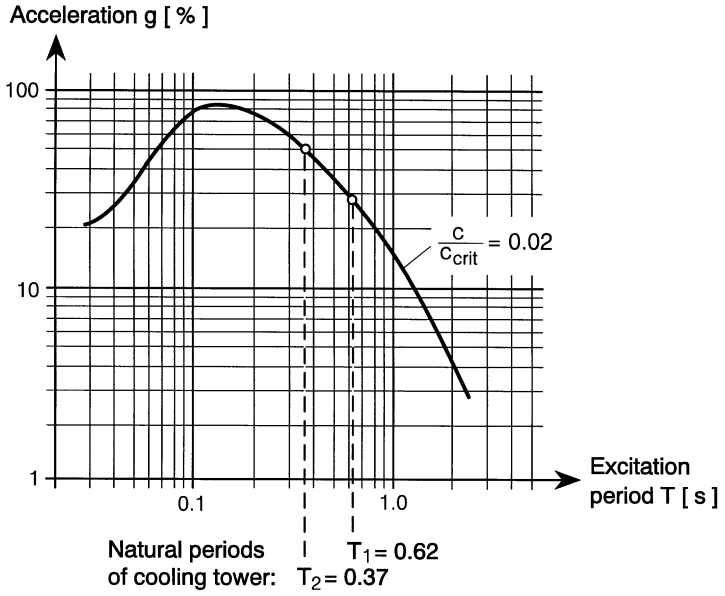

FIGURE 14.36: Seismic response spectrum.

14.8 Construction

Tolerances for tall concrete cooling tower shells have been debated for many years and reasonable values should take into consideration what is achievable and what is measurable. It should be noted that state-of-the-art finite element models are capable of analyzing the as-built shell as well as the design configuration, so that the effects of those irregularities arising during construction, or even those discovered later, may be quantitatively studied and sometimes corrected.

It is recommended that the actual wall thickness be no less than the design thickness and exceed this thickness by not more than 10%. The imperfections of the shell wall middle surface should not exceed one-half of the wall thickness or 10 cm. Deviations from the design geometry occurring

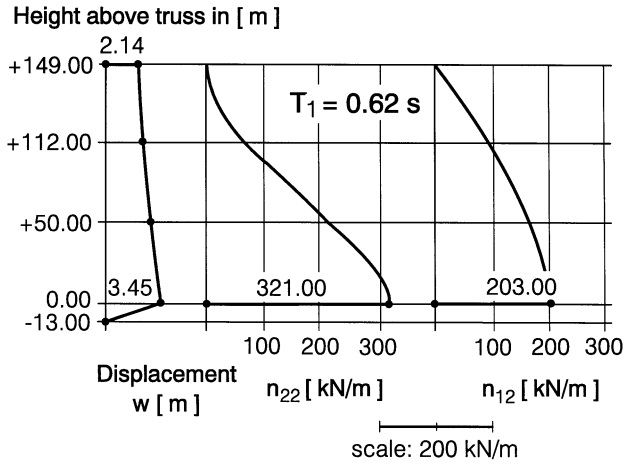

FIGURE 14.37: First axial mode seismic response.

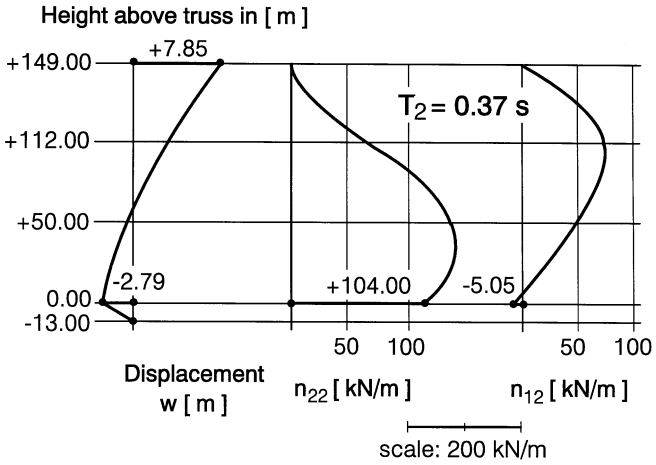

FIGURE 14.38: Second axial mode seismic response.

during the construction should be corrected gradually, limiting the angular change in either direction to 1.5%. The column heads should be within 0.005 times the column height or $\pm$6.0 cm of the design position, and foundation structures should also be within $\pm$6.0 cm of the design location [13].

Formwork and scaffolding systems are generally proprietary and are provided by the constructor. Nevertheless, their influence on the shell quality is of utmost importance and diligent attention of the engineer is required. In general, the system should be designed to provide safety to operating personnel and to produce a sound structure. The working platforms should be designed for realistic loading, and scaffolding systems used for continuous material transport should be designed and built taking into account the resulting loads.

The connections and joints between individual scaffolding units should be designed and built to act independently in case of collapse, so that the loss of one unit would not affect the adjacent units. Furthermore, at least two independent safety devices should be in place to prevent collapse.

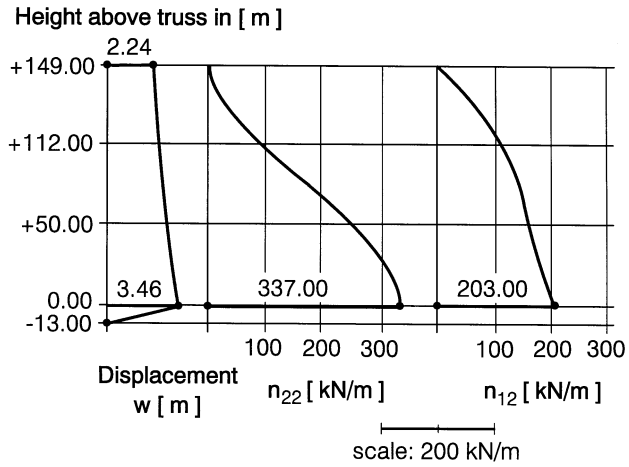

FIGURE 14.39: SRSS superposition of first and second axial modes.

FIGURE 14.40: Column to lintel connection.

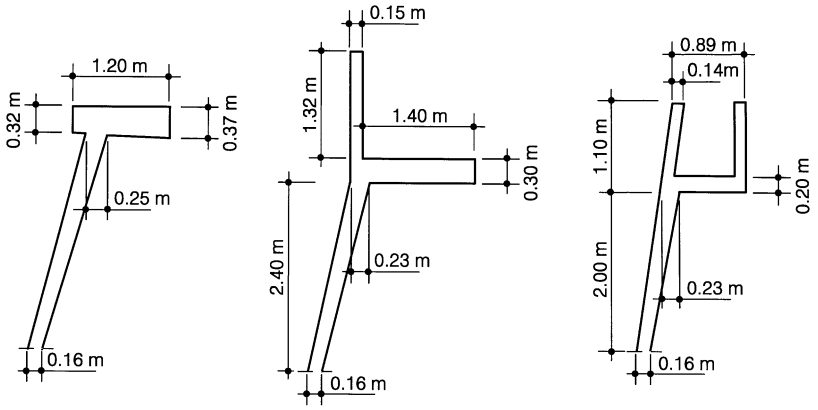

FIGURE 14.41: Suitable forms of the cornice.

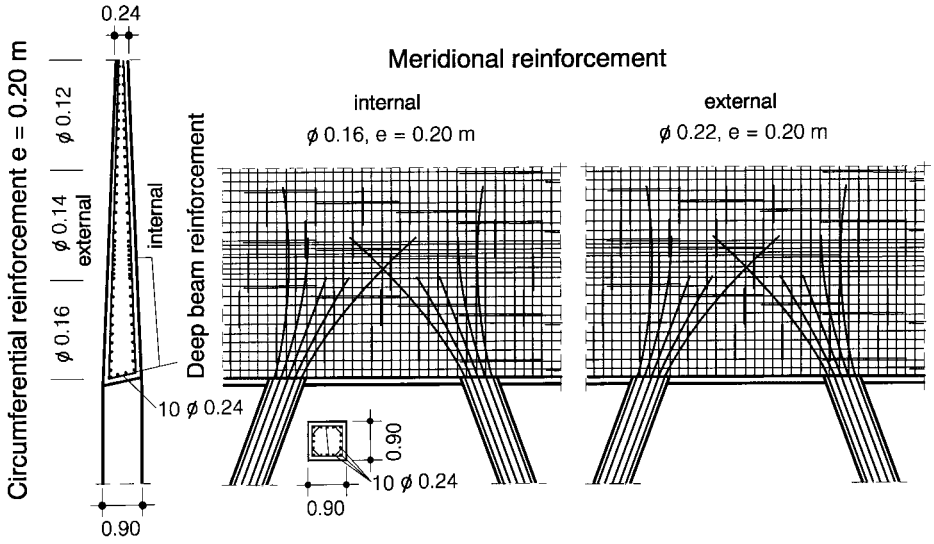

FIGURE 14.42: Lintel reinforcement.

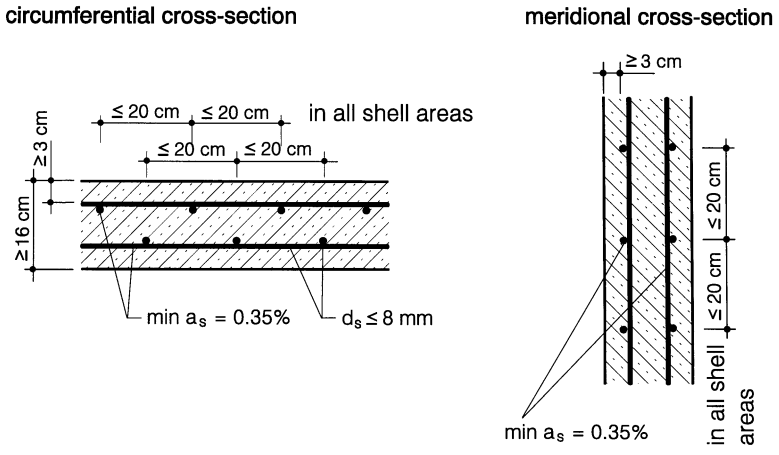

FIGURE 14.43: Important minimum construction values.

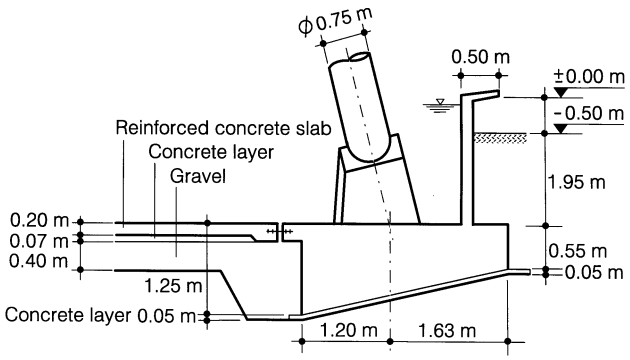

FIGURE 14.44: Flat ring foundation.

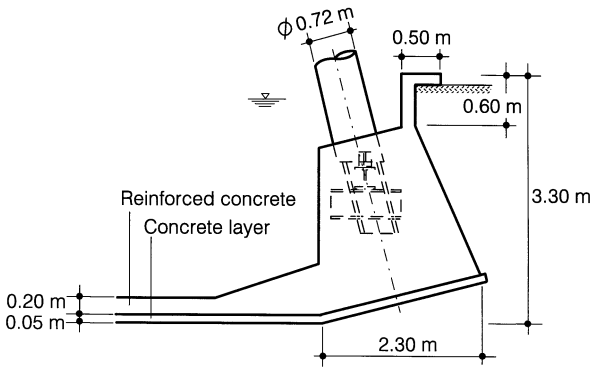

FIGURE 14.45: Ring beam foundation.

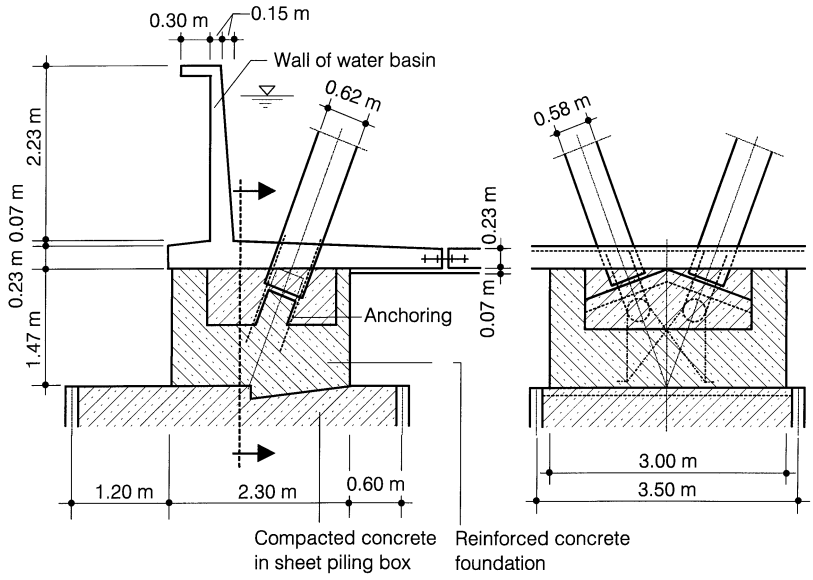

FIGURE 14.46: Individual reinforced concrete foundation on concrete base.

The shell wall should be designed to resist the anchor loads of the scaffolding, based on the strength of the concrete which is expected to be available when the anchors are loaded. Continuous monitoring of the concrete strength during the climbing process is essential.

Cooling tower shells are subjected to a relatively severe environment over their lifetime, which may span several decades, and special care must be taken in order to provide a durable structure. The tower is subjected to the physical loads produced by wind, temperature, and moisture acting on concrete which may still be drying and hardening. Over the lifetime of the structure, it may be exposed to severe frost action in a saturated state, chemical attacks due to noxious substances in the atmosphere and in the water and water vapor, biological attacks due to microorganisms, and possibly additional chemical attacks due to reintroduced cleaned flue gases.

The concrete should be of high-quality approved materials including fly-ash. It should have the following properties:

- High resistance against chemical attacks
- High early strength
- High structural density
- High resistance against frost

The surface finish should be of high quality and the surface should be smooth and essentially free of shrink holes. Air bubbles deeper than 4 mm and unintended surface irregularities at joints should be avoided. The shell should be coated with a curing agent providing a high blocking effect and long durability.

Several single component (acrylate or polyurethene-based) or double component (epoxy resin-based) coating systems are approved worldwide and are in a process of continual improvement. Of utmost importance for any coating is the homogeneity of the applied film between $\geq 200\mu m$ for single and $\geq 300\mu$ for double component systems, since the durability of the complete coating is determined by the thinnest film spots.

References

[1] Abel, J.F. and Gould, P.L. 1981. *Buckling of Concrete Cooling Towers Shells*, ACI SP-67, American Concrete Institute, Detroit, Michigan, pp. 135-160.

[2] ACI-ASCE Committee 334. 1977. Recommended Practice for the Design and Construction of Reinforced Concrete Cooling Towers, *ACI J.*, 74(1), 22-31.

[3] Gould, P.L. 1985. *Finite Element Analysis of Shells of Revolution*, Pitman.

[4] Gould, P.L., Suryoutomo, H., and Sen, S.K. 1974. Dynamic analysis of column-supported hyperboloidal shells, *Earth. Eng. Struct. Dyn.*, 2, 269-279.

[5] Gould, P.L. and Guedelhoefer, O.C. 1988. Repair and Completion of Damaged Cooling Tower, *J. Struct. Eng.*, 115(3), 576-593.

[6] Hayashi, K. and Gould, P.L. 1983. Cracking load for a wind-loaded reinforced concrete cooling tower, *ACI J.*, 80(4), 318-325.

[7] IASS-Recommendations for the Design of Hyperbolic or Other Similarly Shaped Cooling Towers. 1977. Intern. Assoc. for Shell and Space Structures, Working Group No. 3, Brussels.

[8] Krätzig, W.B. and Zhuang, Y. 1992. Collapse simulation of reinforced natural draught cooling towers, *Eng. Struct.*, 14(5), 291-299.

[9] Krätzig, W.B. and Meskouris, K. 1993. Natural draught cooling towers: An increasing need for structural research, *Bull. IASS*, 34(1), 37-51.

[10] Krätzig, W.B. and Gruber, K.P. 1996. Life-Cycle Damage Simulations of Natural Draught Cooling Towers in *Natural Draught Cooling Towers*, Wittek, U. and Krätzig, W., Eds., A.A. Balkema, Rotterdam, 151-158.

[11] Minimum Design Loads for Buildings and Other Structures. 1994. ASCE Standard 7-93, ASCE, New York.
[12] Mungan, I. 1976. Buckling stress states of hyperboloidal shells, *J. Struct. Div.*, ASCE, 102, 2005-2020.
[13] VGB Guideline. 1990. Structural Design of Cooling Towers, VGB-Technical Committee, "Civil Engineering Problems of Cooling Towers", Essen, Germany.

Further Reading

[1] *Proceedings (First) International Symposium on Very Tall Reinforced Concrete Cooling Towers.* 1978. I.A.S.S., E.D.F., Paris, France, November.
[2] Gould, P.L., Krätzig, W.B., Mungan, I., and Wittek, U., Eds. 1984. *Natural Draught Cooling Towers.* Proceedings of the 2nd International Symposium on Natural Draught Cooling Towers, Springer-Verlag, Heidelberg.
[3] *Proceedings Third International Symposium on Natural Draught Cooling Towers.* 1989. I.A.S.S., E.D.F., Paris, France, April.
[4] Wittek, U. and Krätzig, W.B., Eds. 1996. *Natural Draught Cooling Towers.* Proceedings of the 4th International Symposium on Natural Draught Cooling Towers, A.A. Balkema, Rotterdam.
[5] British Standard Institution. 1996. BS 4485, Part 4: British Standard for Water Cooling Towers. Document 96/17117 DC 22.
[6] Syndicat National du Béton Armé et des Techniques Industrialisées. 1996. Regles de conception et de realisation des refrigerants atmospheriques en beton armé, Paris.